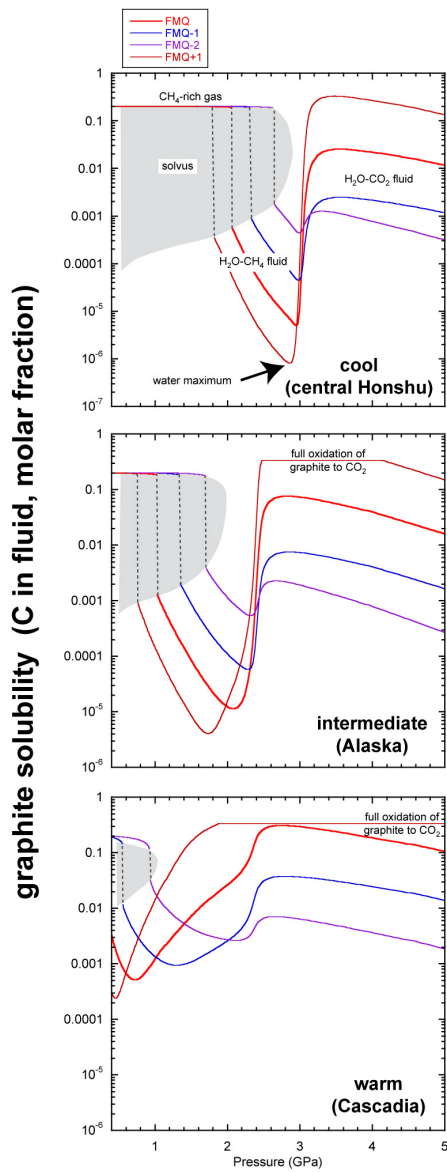
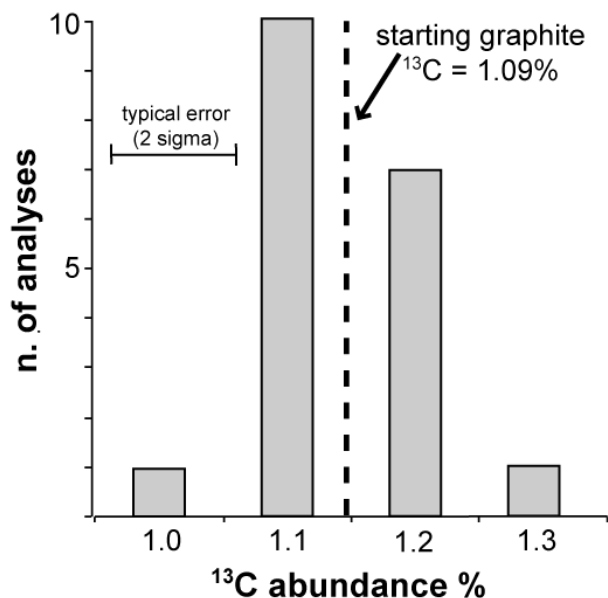


## Supplementary Figure 1



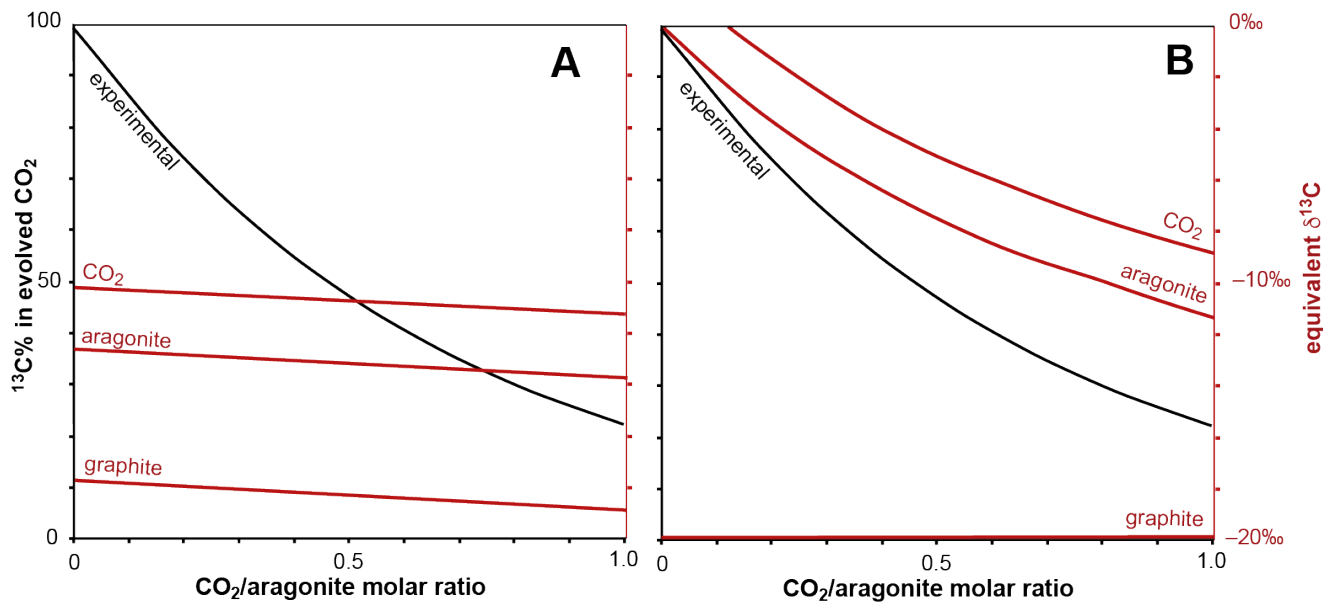
Graphite solubility (molar fraction C) in aqueous fluids buffered at different  $\Delta\text{FMQ}$  conditions. Calculations are performed by conventional thermodynamic modelling of graphite-saturated COH fluids(<sup>1</sup>) for model cool, intermediate and warm subduction regimes. Regardless of geothermal gradient, the carbon content initially decreases with depth to a minimum, then increases over a narrow depth range and remains nearly constant to greater depth. The solubility pattern tracks a transition from CH<sub>4</sub> dominated fluids at shallow depths, and CO<sub>2</sub> dominated fluids at greater depth; the minima occur where the bulk  $X\text{O} = 1/3$  (H<sub>2</sub>O stoichiometry; "water maximum" conditions). Shallow fluid compositions intersect the H<sub>2</sub>O–CH<sub>4</sub> miscibility gap.

## Supplementary Figure 2



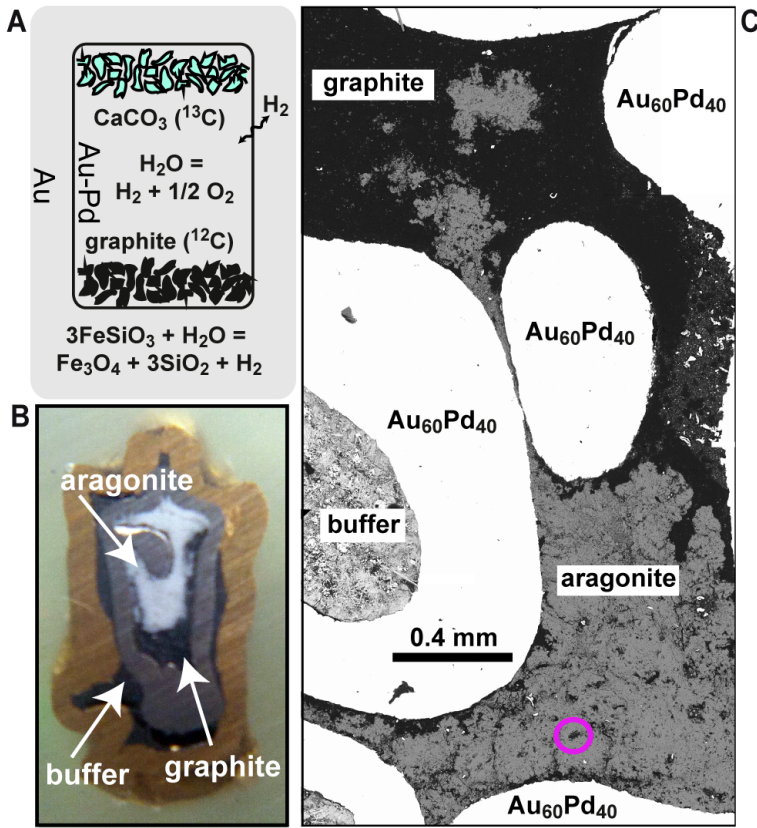
Histogram of the post-quench isotopic composition of graphite. Analyses are performed by means of NanoSIMS and LA-ICP-MS. Dashed line: isotopic composition of the starting graphite (EA-IRMS). Error bar represents typical uncertainty of LA-ICP-MS analyses.

### Supplementary Figure 3



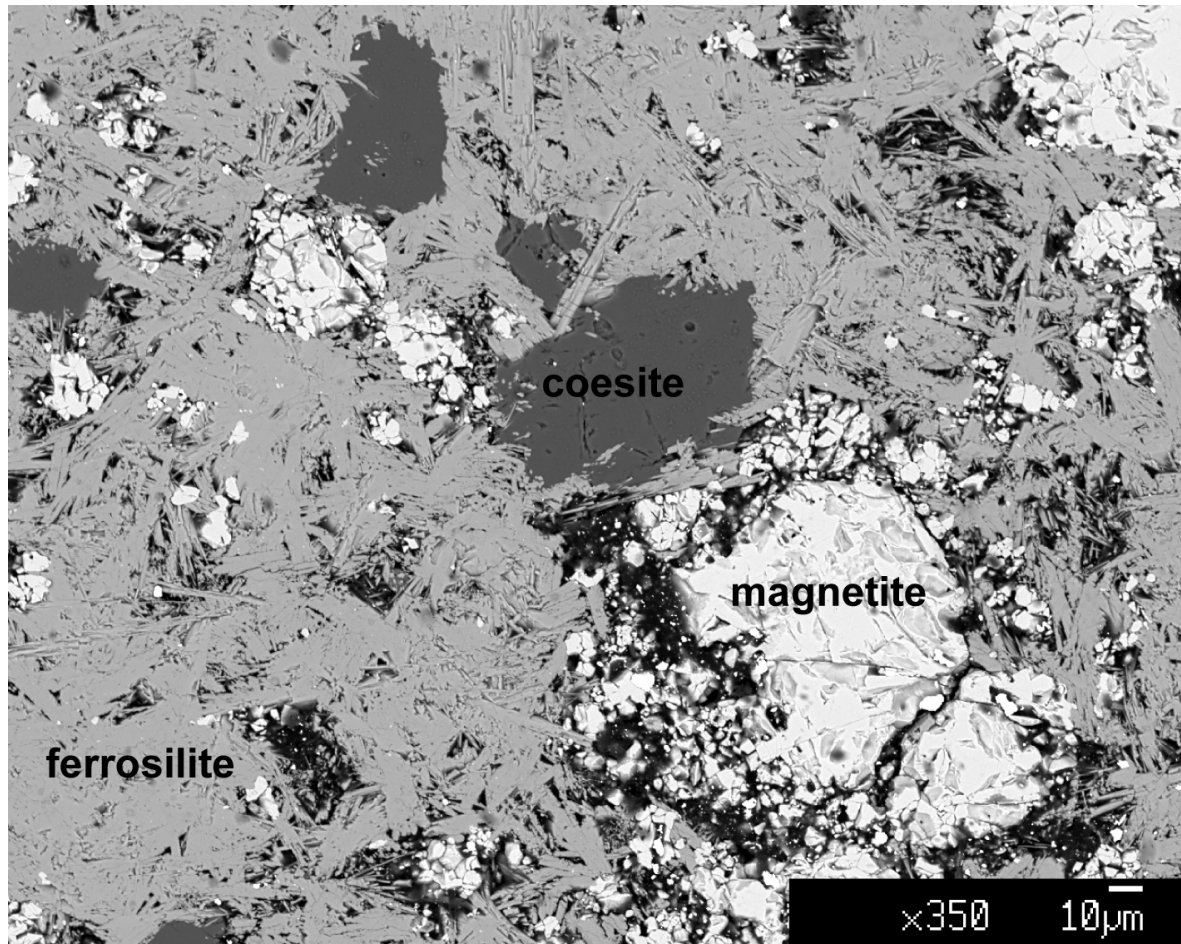
Comparison of the experimental data fit (solid black lines) with conventional isotopic modelling (solid red lines). Modelling is performed assuming  $T = 700^\circ\text{C}$ , room pressure and that  $\delta^{13}\text{C} = 0\text{\textperthousand}$  and  $-20\text{\textperthousand}$  are equivalent to  $^{13}\text{C} = 100\text{\textpercent}$  and  $0\text{\textpercent}$ , respectively.  $\text{CO}_2/\text{CaCO}_3$  molar ratio is displayed in the x-axis. (A) In the conventional isotopic model,  $\text{CO}_2$ , aragonite and graphite can all freely exchange isotopes and reach mass-balance equilibrium. The experimental conditions are replicated with 30  $\mu\text{mol}$  aragonite and progressive oxidation of 166.5  $\mu\text{mol}$  of graphite to  $\text{CO}_2$  from 0  $\mu\text{mol}$  ( $x = 0$ ) to 30  $\mu\text{mol}$  ( $x = 1$ ); (B) graphite is treated as a chemically reactive phase, oxidizing to  $\text{CO}_2$ , but as an isotopically inert phase; in this case only aragonite and  $\text{CO}_2$  can freely exchange isotopes to reach mass-balance equilibrium.

## Supplementary Figure 4



Details of the experimental design. (A) Outline of the typical experimental capsule; in the inner Au–Pd capsule, permeable to H<sub>2</sub>, synthetic graphite and labelled Ca<sup>13</sup>CO<sub>3</sub> interact with excess ultrapure water (~20 wt%). In the outer Au capsule, the buffering assemblage ferrosilite + magnetite + coesite constrains the hydrogen fugacity. The expected *f*O<sub>2</sub> in the inner capsule is ΔFMQ = −0.16. (B) Example of post-quench double capsule (sample COH98) containing the assemblage graphite + aragonite (checked by micro-Raman spectroscopy). Outer gold capsule diameter: 4.5 mm; natural light photograph. (c) Back-scattered electron image of the inner Au–Pd capsule of sample COH92 after NanoSIMS analysis. Size of a typical pit in aragonite is shown within the magenta circle.

**Supplementary Figure 5**



Back-scattered electron image of the buffering assemblage in the outer capsule. The occurrence of ferrosilite + magnetite + coesite is confirmed by electron-microprobe analysis and micro-Raman spectroscopy.

**Supplementary Table 1.** Run table of the experiments performed at 3 GPa–700°C and analyses of volatiles and of bulk after-run aragonite.

**Supplementary Table 2.** Molality of CO<sub>2</sub> in analyzed fluids.

**Supplementary Table 3.** Deep Earth Water thermodynamic modelling of aqueous fluids at the investigated experimental conditions.

**Supplementary Table 4.** Conventional thermodynamic modelling of graphite-saturated fluids (C–O–H system) at the investigated experimental conditions.

**Supplementary Table 5.** Nano-SIMS analyses of graphite and aragonite in sample COH92.

**Supplementary Table 6:** LA-ICP-MS analyses of graphite and aragonite.

**Supplementary Table 7:** Parameters of Equation 6.

**Supplementary Table 8:** Thermal decomposition of oxalic acid di-hydrate and retrieval of the mass-bias QMS correction.

**Supplementary Table 9:** LA-ICP-MS analysis of standard carbonates.

**Supplementary Table 10:** Bulk analyses of labeled reagent and standard carbonates.

**Supplementary Table 1:** Run table of the experiments performed at 3 GPa–700°C and analyses of volatiles and of bulk after-run aragonite.

run	runtime	buffer	starting materials	Ca <sup>13</sup> CO <sub>3</sub> μmol	graphite μmol	Ca <sup>13</sup> CO <sub>3</sub> / graphite	run products (+fluid)	total volatiles μmol	H <sub>2</sub> O	CO <sub>2</sub>	CH <sub>4</sub>	CO <sub>2</sub> mol% <sup>13</sup> C	X CO <sub>2</sub> <sup>a</sup> mol% <sup>13</sup> C <sup>c</sup>	bulk aragonite	CO <sub>2</sub> / Ca <sup>13</sup> CO <sub>3</sub>
COH89	72	fs+mt+coe	Ca <sup>13</sup> CO <sub>3</sub> + H <sub>2</sub> O	55.6	-	-	arag ± cc	62.95	59.50	0.16	0.07	27.1	0.001 <sup>b</sup>	n.m.	0.003
COH99	72	Re+ReO <sub>2</sub>	Ca <sup>13</sup> CO <sub>3</sub> + H <sub>2</sub> O	52.6	-	-	arag ± cc	36.32	31.30	0.14	0.05	42.8	0.002 <sup>b</sup>	n.m.	0.003
COH82	72	fs+mt+coe	Ca <sup>13</sup> CO <sub>3</sub> + Cl-bear. Zr(OH) <sub>4</sub> <sup>d</sup> + H <sub>2</sub> O	91.0	-	-	arag + bdy ± cc	57.84	50.31	2.32	0.05	84.9	0.038 <sup>b,d</sup>	n.m.	0.025
COH83	72	fs+mt+coe	Ca <sup>13</sup> CO <sub>3</sub> + Cl-bear. Zr(OH) <sub>4</sub> <sup>e</sup> + H <sub>2</sub> O	52.4	-	-	arag + bdy ± cc	22.69	18.87	0.97	0.02	86.4	0.042 <sup>b,d</sup>	n.m.	0.018
COH88	72	fs+mt+coe	graphite + H <sub>2</sub> O	-	328.8	-	graph	14.93	6.58	4.81	0.05	1.43	0.422	-	-
COH96	240	fs+mt+coe	graphite + H <sub>2</sub> O	-	331.3	-	graph	20.72	10.37	5.32	0.00	1.11	0.339	-	-
COH170	0.24	fs+mt+coe	graphite + Ca <sup>13</sup> CO <sub>3</sub> + H <sub>2</sub> O	10.2	219.8	0.044	graph + arag ± cc	30.29	26.21	0.70	0.10	62.8	0.026	96.1	0.069
COH186	0.24	fs+mt+coe	graphite + Ca <sup>13</sup> CO <sub>3</sub> + H <sub>2</sub> O	29.6	194.0	0.132	graph + arag ± cc	14.35	11.69	0.34	0.00	52.9	0.028	97.2	0.012
COH106	2.4	fs+mt+coe	graphite + Ca <sup>13</sup> CO <sub>3</sub> + H <sub>2</sub> O	24.9	183.2	0.120	graph + arag ± cc	21.10	18.06	0.71	0.01	80.5	0.038	95.8	0.028
COH98	24	fs+mt+coe	graphite + Ca <sup>13</sup> CO <sub>3</sub> + H <sub>2</sub> O	29.5	174.0	0.145	graph + arag ± cc	22.94	17.88	2.51	0.02	88.4	0.123	88.1	0.085
COH92	72	fs+mt+coe	graphite + Ca <sup>13</sup> CO <sub>3</sub> + H <sub>2</sub> O	28.3	188.1	0.131	graph + arag ± cc	28.44	21.28	3.93	0.02	81.7	0.156	89	0.139
COH97	240	fs+mt+coe	graphite + Ca <sup>13</sup> CO <sub>3</sub> + H <sub>2</sub> O	29.2	190.6	0.133	graph + arag ± cc	26.53	18.37	3.66	b.d.l.	82.2	0.166	82.9	0.125
COH171	0.24	fs+mt+coe	Ca <sup>13</sup> CO <sub>3</sub> + OAD (0.3 mg)	37.8	-	-	arag ± cc	7.56	1.74	3.47	0.00	84.1	0.666	83.8	0.092
COH178	72	fs+mt+coe	Ca <sup>13</sup> CO <sub>3</sub> + OAD (0.3 mg)	40.2	-	-	arag ± cc	11.07	3.89	5.27	0.04	79.9	0.575	80.8	0.131
COH184	72	fs+mt+coe	Ca <sup>13</sup> CO <sub>3</sub> + OAD (0.3 mg)	29.9	-	-	arag ± cc	11.02	4.48	2.82	0.00	84.3	0.386	86.7	0.094
COH185	72	fs+mt+coe	Ca <sup>13</sup> CO <sub>3</sub> + OAD (2 mg)	29.8	-	-	arag ± cc	41.52	17.08	17.99	0.05	54.7	0.513	55.3	0.604

a:  $X \text{ CO}_2 = \text{CO}_2 / (\text{H}_2\text{O} + \text{CO}_2)_{\text{molar}}$

b: considering only <sup>13</sup>CO<sub>2</sub>

c: total decomposition by HCl + QMS analysis of evolved CO<sub>2</sub>

d: chlorine in Zr(OH)<sub>4</sub> = 0.6 wt%; calculated final fluid Cl concentration = 0.89 mol Cl/kgH<sub>2</sub>O

e: chlorine in Zr(OH)<sub>4</sub> = 0.6 wt%; calculated final fluid Cl concentration = 0.54 mol Cl/kgH<sub>2</sub>O

n.m.: not measured

b.d.l.: below detection limit

fs: ferrosilite; mt: magnetite; coe:coesite; arag: aragonite; cc: calcite; graph: graphite; bdy: baddeleyite; OAD: oxalic acid di-hydrate

**Supplementary Table 2: Molality of CO<sub>2</sub> in analyzed fluids.**

Run	mol <sup>13</sup> CO <sub>2</sub> / kgH <sub>2</sub> O	mol CO <sub>2(TOT)</sub> / kgH <sub>2</sub> O
COH89	0.041	-
COH99	0.108	-
COH82	2.169	-
COH83	2.460	-
COH88	-	39.99
COH96	-	28.16
COH170	-	1.482
COH186	-	1.617
COH106	-	2.167
COH98	-	7.794
COH92	-	10.26
COH97	-	11.05
COH171	-	110.6
COH178	-	75.25
COH184	-	34.86
COH185	-	58.46



**Supplementary Table 3: Deep Earth Water thermodynamic modelling of aqueous fluids at the investigated experimental conditions.**

saturated phases	aragonite	graphite	graphite+aragonite
P (GPa)	3	3	3
T (°C)	700	700	700
log(fH <sub>2</sub> /1 bar)	2.195	2.195	2.195
pH	5.090	2.210	4.200
X CO <sub>2</sub> =[CO <sub>2</sub> (AQ)/(H <sub>2</sub> O+CO <sub>2</sub> (AQ)]	0.0002	0.305	0.284
C bulk solubility (molality)	0.1205	24.40	24.05
<i>predicted species (decreasing molality)</i>			
OH-	1.12E-01	CO <sub>2</sub> (AQ)	2.44E+01
CA(HCO <sub>3</sub> ) <sup>+</sup>	8.94E-02	H+	6.78E-03
CA(OH) <sup>+</sup>	1.37E-02	CO(AQ)	5.67E-03
CA(HCOO) <sup>+</sup>	1.10E-02	HCO <sub>3</sub> -	5.39E-03
CO <sub>2</sub> (AQ)	8.80E-03	HCOOH	4.15E-03
HCO <sub>3</sub> -	6.24E-03	HCOO-	1.32E-03
CACO <sub>3</sub> (AQ)	3.50E-03	CH <sub>4</sub> (AQ)	3.19E-04
CA++	2.97E-03	H <sub>2</sub> (AQ)	1.77E-04
HCOO-	1.15E-03	OH-	8.98E-05
CO <sub>3</sub> --	2.46E-04	CH <sub>3</sub> COOH	3.67E-05
H <sub>2</sub> (AQ)	1.77E-04	CH <sub>3</sub> CH <sub>2</sub> COO-	7.38E-07
H+	1.12E-05	METHANOL(AQ)	7.20E-07
CO(AQ)	3.95E-06	ETHANOL(AQ)	3.00E-07
HCOOH	3.84E-06	CH <sub>3</sub> COO-	2.24E-07
CH <sub>4</sub> (AQ)	1.67E-07	CO <sub>3</sub> --	1.45E-07
METHANOL(AQ)	5.02E-10	ETHANE(AQ)	1.17E-07
CH <sub>3</sub> COO-	1.03E-10	CH <sub>3</sub> CH <sub>2</sub> COOH	1.06E-07
CH <sub>3</sub> COOH	1.79E-11	ETHYLENE(AQ)	4.48E-09
CH <sub>3</sub> CH <sub>2</sub> COO-	1.77E-13	PROPANE(AQ)	8.26E-11
ETHANOL(AQ)	1.10E-13	O <sub>2</sub> (AQ)	1.25E-20
ETHANE(AQ)	3.21E-14	PROPANOL	5.76E-25
ETHYLENE(AQ)	1.23E-15		
CH <sub>3</sub> CH <sub>2</sub> COOH	2.70E-17		
O <sub>2</sub> (AQ)	2.20E-20		
PROPANE(AQ)	1.20E-20		
PROPANOL	1.107E-34		
<i>abundances among carbon-bearing species</i>			
% Ca(HCO <sub>3</sub> ) <sup>+</sup>	74.27	-	3.70
% CO <sub>2</sub> (AQ)	7.31	99.93	91.40

**Supplementary Table 4: Conventional thermodynamic modelling of graphite-saturated fluids (C–O–H system) at the investigated experimental conditions.**

$P$ (GPa), $T$ (° C)	3, 700
buffer	ferrosilite + magnetite + coesite
$\log(f\text{O}_2/1 \text{ bar})$ outer capsule <sup>a</sup>	-13.21
$\log(f\text{H}_2/1 \text{ bar})$ outer capsule = inner capsule <sup>b</sup>	2.195
$\log(f\text{O}_2/1 \text{ bar})$ inner capsule <sup>c</sup>	-13.36
$X\text{CO}_2$ <sup>c</sup>	0.303
$\log(f\text{O}_2/1 \text{ bar})^{\text{FMQ},\text{d}}$	-13.97
$\Delta\text{FMQ}$ <sup>e</sup> inner capsule	+0.61

<sup>a</sup> $\log(f\text{O}_2/1 \text{ bar})$  of the buffering assemblage  $3 \text{ FeSiO}_3 + 0.5 \text{ O}_2 = \text{Fe}_3\text{O}_4 + 3 \text{ SiO}_2$  (coesite), retrieved using the Perple\_X package and the hp02ver.dat database.

<sup>b</sup> retrieved using the routine "fluids" of the Perple\_X package (H–O HSMRK/MRK hybrid EoS).

<sup>c</sup>retrieved on the basis of constant  $\log(f\text{H}_2/1 \text{ bar})$  using the routine "fluids" of the Perple\_X package (GCOH-fluid MRK).

<sup>d</sup> $\log(f\text{O}_2/1 \text{ bar})$  of the metastable assemblage  $3 \text{ Fe}_2\text{SiO}_4 + \text{O}_2 = 2 \text{ Fe}_3\text{O}_4 + 3 \text{ SiO}_2$  (quartz).

<sup>e</sup>  $\Delta\text{FMQ} = \log(f\text{O}_2/1 \text{ bar})^{\text{sample}} - \log(f\text{O}_2/1 \text{ bar})^{\text{FMQ}}$

**Supplementary Table 5:** Nano-SIMS analyses of graphite and aragonite in sample COH92.

<b>Filename</b>	<b><math>^{13}\text{C}</math> mol%</b>	<b>2 sigma</b>
<i>graphite</i>		
analysis #1	1.119	0.006
analysis #2	1.141	0.003
analysis #3	1.171	0.003
analysis #4	1.181	0.003
<i>aragonite</i>		
analysis #1	4.101	0.006
analysis #2	8.81	0.04
analysis #3	10.12	0.04
analysis #4	13.04	0.05
analysis #5	20.3	0.2
analysis #6	24.0	0.8
analysis #7	27.3	0.2
analysis #8	28.6	0.3
analysis #9	29.1	0.2
analysis #10	31	1
analysis #11	31.6	0.1
analysis #12	32.4	0.7
analysis #13	41.4	0.8
analysis #14	41.5	0.7
analysis #15	84.0	0.8

**Supplementary Table 6: LA-ICP-MS analyses of graphite and a**

	<sup>13</sup> C mol%	2 sigma
<i>graphite</i>		
COH106_1	1.4	0.2
COH106_2	1.5	0.2
COH106_3	1.2	0.1
COH98_1	1.2	0.1
COH98_2	1.1	0.1
COH92_1	1.1	0.1
<i>aragonite</i>		
COH106_1	65.2	0.7
COH106_2	71.5	0.7
COH106_3	70.5	0.7
COH106_4	67.8	0.7
COH106_5	70.6	0.7
COH106_6	55.5	0.6
COH106_7	58.9	0.6
COH106_8	76.9	0.8
COH106_9	74.9	0.7
COH106_10	76.4	0.8
COH106_11	58.8	0.6
COH106_12	59.0	0.6
COH106_13	81.6	0.8
COH106_14	71.6	0.7
COH106_15	71.9	0.7
COH98_1	45.5	0.5
COH98_2	45.3	0.5
COH98_3	46.2	0.5
COH98_4	47.0	0.5
COH92_1	36.2	0.4
COH92_2	27.6	0.3
COH92_3	38.7	0.4
COH92_4	38.6	0.4
COH92_5	42.0	0.4
COH92_6	37.9	0.4
COH92_7	38.4	0.4
COH92_8	43.7	0.4
COH92_9	49.8	0.5
COH92_10	41.0	0.4
COH92_11	45.9	0.5
COH97_1	36.5	0.4
COH97_2	98	1
COH97_3	88.9	0.9
COH97_4	55.4	0.6
COH97_5	38.0	0.4
COH97_6	73.7	0.7
COH97_7	60.5	0.6
COH97_8	53.1	0.5
COH97_9	52.2	0.5
COH97_10	57.2	0.6
COH97_11	63.0	0.6

**Supplementary Table 7: Parameters of Equation 6.**

Independent variable	Parameter estimate	sigma
1	4.71676	0.0507989
WAR	-2.87021	0.0494956
$\Delta\text{FMQ}$	-3.00212	0.163084
$\Delta\text{FMQ}^2$	2.15874	0.238246
$\Delta\text{FMQ}^3$	-2.08921	0.118716
$\Delta\text{FMQ} \times \text{WAR}$	0.294843	0.0586424
$\text{WAR}^2$	1.02176	0.0267483
$\text{WAR}^3$	-0.12774	0.00443806
$\Delta\text{FMQ}^2 \times \text{WAR}$	-1.02538	0.0513343
$\text{WAR}^{-2}$	0.0030557	0.00010255

WAR=water/aragonite molar ratio.

$$\Delta\text{FMQ} = \log(f\text{O}_2/1 \text{ bar})^{\text{sample}} - \log(f\text{O}_2/1 \text{ bar})^{\text{FMQ}}$$

**Supplementary Table 8: Thermal decomposition of oxalic acid di-hydrate and retrieval of the mass-bias QMS correction factor.**

	<sup>12</sup> C-OAD mg	<sup>13</sup> C-OAD mg	predicted <sup>13</sup> C/ <sup>12</sup> C	predicted <sup>13</sup> C abundance mol%	integrated peak channel 44	integrated peak channel 45	ratio 45/44	ratio 45 <sub>corr</sub> <sup>a</sup> /44	<sup>13</sup> C abundance %
regular OAD	3.6	0	0.013	1.25	5.53E-06	7.02E-08	0.013	-	1.29
labeled <sup>13</sup> C-OAD	0	9.91	191.283	99.5	2.86E-07	5.47E-05	191.283	-	99.5
mix 1	5.55	5.11	0.922	48.0	7.45E-06	6.38E-06	0.856	0.881	46.9
mix 2	7.52	1.53	0.214	17.6	8.79E-06	2.40E-06	0.273	0.281	22.0
mix 3	0.72	9.06	11.729	92.1	3.92E-06	4.45E-05	11.364	11.705	92.1
<u>test_AA8</u>	0.56	0.86	1.52	60.4	0.00	0.00	1.35	1.39	58.1

OAD: oxalic acid di-hydrate

a: using correction factor 1.03 for channel 45, corresponding to a regression line through mix1–mix2–mix3 with  $R^2=0.99993$

**Supplementary Table 9: LA-ICP-MS of standard carbonates.**

	$^{13}\text{C}$ mol%	2 sigma
<i>natural calcite</i>		
natural_calcite_1	1.07	0.05
natural_calcite_2	1.09	0.05
natural_calcite_3	1.15	0.06
natural_calcite_4	1.12	0.06
natural_calcite_5	1.10	0.05
<i>synthetic calcite</i>		
synthetitc_calcite_1	43.9	0.4
synthetitc_calcite_2	43.7	0.4
synthetitc_calcite_3	44.4	0.4

synthetic calcite is precipitated from mixed  $^{12}\text{C}$ - $^{13}\text{C}$   $\text{Na}_2\text{CO}_3$  solutions.

**Supplementary Table 10: Bulk analyses of labelled reagent and standard carbonates.**

	integrated peak channel 44	integrated peak channel 45	ratio 45/44	ratio $45_{corr}^a/44$	$^{13}\text{C}$ abundance mol%
synthetic $^{13}\text{C}$ calcite	6.83E-08	1.18E-05	173	178	99.4
precipitated ( $^{12}\text{C}$ , $^{13}\text{C}$ ) synthetitic calcite	4.45E-06	3.36E-06	0.755	0.778	43.8
natural-abundance calcite	5.62E-06	6.22E-08	0.0111	0.0114	1.13

a: using correction factor 1.03 for the integrated peak of channel 45.